

See discussions, stats, and author profiles for this publication at: <https://www.researchgate.net/publication/230762346>

# Potential methane reservoirs beneath Antarctica

Article in *Nature* · August 2012

DOI: 10.1038/nature11374 · Source: PubMed

CITATIONS

84

READS

245

13 authors, including:



**Jemma L. Wadham**  
University of Bristol

131 PUBLICATIONS 2,685 CITATIONS

[SEE PROFILE](#)



**Sandra Arndt**  
University of Bristol

48 PUBLICATIONS 1,341 CITATIONS

[SEE PROFILE](#)



**Slawek Tulaczyk**  
University of California, Santa Cruz

204 PUBLICATIONS 5,360 CITATIONS

[SEE PROFILE](#)



**Marek Stibal**  
Charles University in Prague

58 PUBLICATIONS 1,574 CITATIONS

[SEE PROFILE](#)

Some of the authors of this publication are also working on these related projects:



Quantification of clastic sediment sources [View project](#)



Coupled Terrestrial-Aquatic Climate Impacts on High Arctic Watersheds: Using the Lake Hazen Watershed as a Sentinel for Change [View project](#)

# Potential methane reservoirs beneath Antarctica

J. L. Wadham<sup>1</sup>, S. Arndt<sup>1,2</sup>, S. Tulaczyk<sup>3</sup>, M. Stibal<sup>1</sup>, M. Tranter<sup>1</sup>, J. Telling<sup>1</sup>, G. P. Lis<sup>1</sup>, E. Lawson<sup>1</sup>, A. Ridgwell<sup>1</sup>, A. Dubnick<sup>4</sup>, M. J. Sharp<sup>3</sup>, A. M. Anesio<sup>1</sup> & C. E. H. Butler<sup>1</sup>

**Once thought to be devoid of life, the ice-covered parts of Antarctica are now known to be a reservoir of metabolically active microbial cells and organic carbon<sup>1</sup>. The potential for methanogenic archaea to support the degradation of organic carbon to methane beneath the ice, however, has not yet been evaluated. Large sedimentary basins containing marine sequences up to 14 kilometres thick<sup>2</sup> and an estimated 21,000 petagrams (1 Pg equals 10<sup>15</sup> g) of organic carbon are buried beneath the Antarctic Ice Sheet. No data exist for rates of methanogenesis in sub-Antarctic marine sediments. Here we present experimental data from other subglacial environments that demonstrate the potential for overridden organic matter beneath glacial systems to produce methane. We also numerically simulate the accumulation of methane in Antarctic sedimentary basins using an established one-dimensional hydrate model<sup>3</sup> and show that pressure/temperature conditions favour methane hydrate formation down to sediment depths of about 300 metres in West Antarctica and 700 metres in East Antarctica. Our results demonstrate the potential for methane hydrate accumulation in Antarctic sedimentary basins, where the total inventory depends on rates of organic carbon degradation and conditions at the ice-sheet bed. We calculate that the sub-Antarctic hydrate inventory could be of the same order of magnitude as that of recent estimates made for Arctic permafrost. Our findings suggest that the Antarctic Ice Sheet may be a neglected but important component of the global methane budget, with the potential to act as a positive feedback on climate warming during ice-sheet wastage.**

The production of methane (CH<sub>4</sub>) by methanogenic archaea is common across many sub-surface environments, including the deep ocean<sup>4–8</sup>, permafrost<sup>9</sup> and lake sediments<sup>10–12</sup> and is promoted by the presence of a suitable organic carbon (OC) substrate and an absence of higher-energy-yielding electron acceptors (for example, O<sub>2</sub> and SO<sub>4</sub><sup>2–</sup>) with which to degrade organic matter. The release of this biogenic methane to the atmosphere is important in driving changes in global climate on geological, millennial and centenary timescales<sup>13</sup>. ‘Geological’ methane, produced largely via thermogenic processes in the deep sub-surface, supplements the biogenic component<sup>13</sup>. This methane may be generated via the thermal breakdown of organic matter and by inorganic synthesis and outgassing from the mantle. The recent discovery that sub-ice-sheet environments are likely to be anoxic<sup>14</sup>, are host to micro-organisms<sup>15</sup> and may contain significant reservoirs of OC identifies them as favourable sites for methanogenesis. Research has so far focused upon the potential biological conversion of overridden OC to methane beneath the Northern Hemisphere Pleistocene ice sheets<sup>14,16</sup>, where high-pressure and low-temperature conditions permit methane to accumulate as hydrate. Methane accumulation beneath the Antarctic Ice Sheet has not yet been evaluated, despite the presence of extensive and deep sedimentary basins containing viable microbial populations<sup>15</sup> and OC available for conversion to methane.

Several factors suggest that there should be methane present beneath the Antarctic Ice Sheet. Geophysical data indicate extensive Antarctic sedimentary basins (ASBs) beneath the West and East

Antarctic Ice Sheets (WAIS and EAIS), containing sedimentary drapes of up to 14 km in thickness (Supplementary Table 1). Many of these basins are located around the Antarctic periphery, but penetrate several 100–1,000 km into the Antarctic interior and are associated with the onset of accelerated motion in ice streams and their tributaries (Supplementary Information 1). The inferred origin of these sediments is marine, glaci-marine and crustal sedimentary sources (Supplementary Table 1). Melting conditions beneath about half of the ice sheet mean that sediments contain liquid water beneath the ice cover<sup>17,18</sup>. The widespread presence of either dissolved methane or geochemical evidence for methanogenesis in marine cores, rock cores and seeps around the Antarctic margin indicates that OC is commonly cycled to methane in ocean margin basins (Supplementary Information 1). It is reasonable to expect similar processes to prevail beneath the ice. We therefore evaluated the potential for methane generation and release from sedimentary basins buried beneath the Antarctic Ice Sheet.

We calculate that 50% of the WAIS (10<sup>6</sup> km<sup>2</sup>) and 25% of the EAIS (2.5 × 10<sup>6</sup> km<sup>2</sup>) overlie ASBs, where areas of the bed substantially below sea level have been inferred to contain thick marine sediments (Supplementary Information 1). Despite the difference in overriding substrate (for example, an ice cap rather than an ocean water column or atmosphere), comparable processes should operate in both ASBs, sub-seafloor sediments and the terrestrial deep biosphere. Typically, ASBs are capped by subglacial till (Fig. 1a). Oxygen supply from the release of air bubbles in melting basal ice is small and quenched by sulphide oxidation and microbial respiration in surface till, such that subglacial sediments are largely anoxic. Hence, most degradation of organic matter occurs anaerobically, first using NO<sub>3</sub><sup>–</sup>, next Fe(III) and SO<sub>4</sub><sup>2–</sup> as electron acceptors<sup>14</sup>, and ultimately via disproportionation into CO<sub>2</sub> and methane<sup>16</sup>. Beneath the till layer, the sediment biogeochemical profile should resemble that of circum-Antarctic marine or terrestrial sediments at the onset of glaciation. In the former case, marine sulphate concentrations would be expected to decrease within the upper 150 m of the sediment column, beyond which methanogenesis is the dominant terminal process for OC decomposition<sup>19</sup> (Fig. 1). We calculate that about 21,000 petagrams of carbon (PgC) was present in ASBs at the time of ice-sheet initiation (Supplementary Information 3e). This is more than ten times the magnitude of OC stocks in northern permafrost regions<sup>20</sup> and parallels the order of magnitude estimates made for reactive carbon in ocean sediments (assuming a 10% reactive OC content for ASBs)<sup>21</sup>. Subglacial ASBs thus constitute a substantial reservoir of OC that has been previously overlooked.

No data exist for rates of methanogenesis in sub-Antarctic marine and terrestrial sediments, but new experimental data from other subglacial environments demonstrate the potential for overridden organic matter beneath glacial systems to produce methane (see Supplementary Information). We obtained subglacial samples derived from the impurity-rich (silty) sections of basal ice exposed at the margins of the Greenland Ice Sheet and in Antarctic and Canadian Arctic glaciers. These samples display concentrations of OC an order of magnitude less (0.07–0.5%) than those recorded in the sub-seafloor, largely owing to inclusions of minerogenic glacial till with the overridden organic

<sup>1</sup>School of Geographical Sciences, University of Bristol, Bristol BS8 1SS, UK. <sup>2</sup>Department of Earth Sciences – Geochemistry, Utrecht University, 3508 Utrecht, The Netherlands. <sup>3</sup>Earth and Planetary Sciences Department, University of California, Santa Cruz, California 95064, USA. <sup>4</sup>Department of Earth and Atmospheric Sciences, University of Alberta, Edmonton T6G 2E3, Canada.

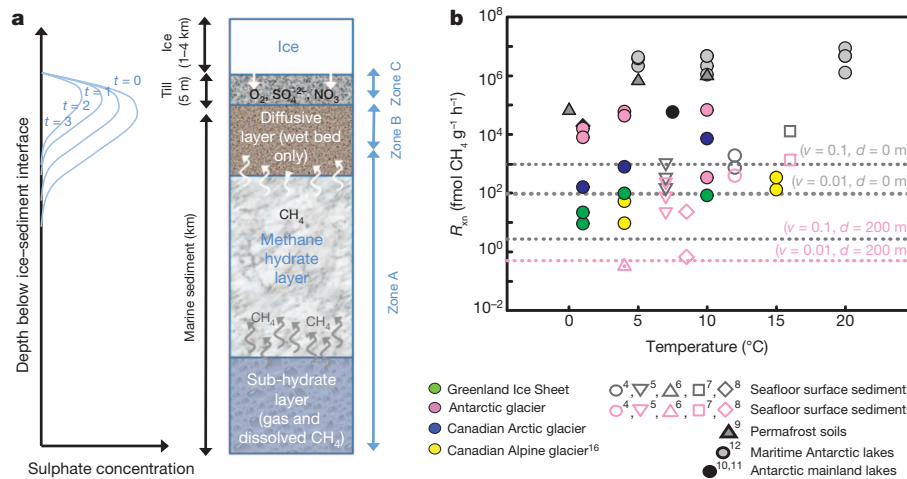


**Figure 1 | Methane production in sub-Antarctic sediments.** **a**, A conceptual model of biogeochemical processes in a sub-Antarctic marine sediment/till complex, indicating three main zones and assuming non-frozen basal conditions. Zone A is the methane production zone (after 16 kyr of glaciation), zone B is the sulphate reduction/anaerobic oxidation of methane zone (during the first 16 kyr of glaciation) and zone C is the sulphide oxidation (oxic/anoxic)/nitrate reduction zone. White arrows indicate methane diffusion. In parts of the ice sheet where frozen basal conditions prevail, zone A is likely to extend to the ice/sediment interface. The graph on the left also indicates the likely evolution of sulphate concentrations in the upper part of the marine sediment/till complex over time ( $t$  values indicate arbitrary, increasing periods of time), as

matter<sup>4</sup>. Order-of-magnitude contrasts in rates of methanogenesis are observed, a reflection of large differences in OC bioavailability. The high rates of methanogenesis in Canadian Arctic ( $10^2$ – $10^3$  fmol CH<sub>4</sub> per gram dry weight of subglacial sediment per hour) and Antarctic sediments ( $10^3$ – $10^4$  fmol CH<sub>4</sub> g<sup>-1</sup> h<sup>-1</sup>), which include overridden lake sediments, are consistent with the known availability of simple polymers and OC in lacustrine material<sup>22</sup>, and approach values reported from perennially ice-covered Antarctic lakes<sup>10,11</sup>. Very low rates of methanogenesis (9–93 fmol CH<sub>4</sub> g<sup>-1</sup> h<sup>-1</sup> at 1–10 °C) in Greenland Ice Sheet sediments align with those reported for the Robertson Glacier in Canada (9–51 fmol g<sup>-1</sup> h<sup>-1</sup> at 4 °C; ref. 16), both reflecting the more recalcitrant nature of carbon in overridden palaeosols (Fig. 1b). Remarkably, these minimum rates of activity align closely with rates of methane production reported in deep (>150 m) sub-sea-floor sediments (Fig. 1b).

We used a well-established one-dimensional numerical hydrate model, developed to model methane hydrate accumulation beneath the sea floor<sup>3</sup>. We assume that the seaward extent of these ASBs is the present-day grounding line and that the WAIS and EAIS were present to an extent similar to that of the present day one million years (Myr) ago and 30 Myr ago, respectively. The 1-Myr value is the maximum estimate indicated by recent modelling (Supplementary Information 1). The potential to generate methane in ASBs depends critically upon the rate at which methane can be produced *in situ* relative to the rates at which it is lost during glaciation. Methane production rates in the model ( $R_{\text{xn}}(z,t)$ ) are scaled to decreasing organic matter quality with sediment age, and hence depth, using a reactive continuum model<sup>23</sup>. Key parameters in the continuum model are the percentage surface total OC content of sediments (TOC(time  $t=0$  yr, depth  $d=0$  m), and the reactivity parameter  $\nu$ . The exponent  $\nu$  determines the shape of the vertical distribution of organic matter reactivity with depth (Supplementary Information 2f, Supplementary Figs 2 and 4).

Modelling in initial simulations assumes that advective gas transport (for example, via fluid flow or venting) is likely to be minimal at the ice-sheet bed (Supplementary Information 2f). Two end-member scenarios are modelled for the surface boundary condition in these cases: (1) the maximum flux scenario (methane loss occurs via diffusion at the sediment surface into the overlying subglacial water system), and (2)

the sulphate pool is depleted by methane oxidation and sulphate reduction (where  $t=3$  is of the order of 10 kyr). **b**, Comparison of rates of methane production ( $R_{\text{xn}}$ , in units of fmol CH<sub>4</sub> per gram dry weight of sediment per hour) measured experimentally for subglacial sediments (this paper) and other anoxic environments. For comparison, we also plot  $R_{\text{xn}}$  values used in the modelling for two parameter sets for surface sediments (depth  $d=0$ ; grey symbols) and sediments exceeding 200 m depth (pink symbols) and for  $\nu=0.1$  and  $\nu=0.01$  (where  $\nu$  is the reactivity parameter in the OC degradation model, with high  $\nu$  values indicating high organic matter reactivity). (The percentage total OC content of sediments, TOC(0,0) = 1%.)

the zero flux scenario (closed-system conditions arising from either frozen basal conditions or saturation of the overlying water film with methane). We apply the zero flux scenario over 20% and 10% of the EAIS and WAIS basins respectively, based on the distribution of frozen basal conditions above ASBs<sup>17</sup> (Supplementary Information 1, and Fig. 2).

In sub-sea-floor sediments, sulphate oxidizes up to 90% of the methane diffusing into the sulphate reduction zone by the anaerobic oxidation of methane (zone B, Fig. 1a)<sup>24</sup>. A key difference between sub-sea-floor and sub-Antarctic sediments is that, whereas the former have a large overlying sulphate reservoir from sea water, subglacial sediments have a relatively small and finite sulphate reserve derived from the original marine material and ongoing sulphide oxidation (Supplementary Information 2e). We calculate that an initial sulphate pool in the subglacial sediment/till complex reduces to zero over about 16,000 years (16 kyr) by anaerobic oxidation of methane coupled to sulphate reduction (Supplementary Information 1, Fig. 1a). Hence, all model simulations assume that methanogenesis cannot occur in the upper 150 m of the sediment column during the first 16 kyr.

The potential to release subglacial methane rapidly following deglaciation is contingent upon whether methane generated in sediments during glaciation can be trapped as methane hydrate or as free gas beneath a hydrate layer. Hydrate forms when dissolved methane concentrations are in excess of saturation within the gas hydrate stability zone (GHSZ), where the latter spans the upper 270 m and 670 m of a ~1-km-deep sediment column beneath the WAIS and EAIS respectively (Fig. 3). The thinner GHSZ beneath the WAIS reflects the higher geothermal heat flux and thinner ice, both of which affect hydrate stability.

Model sensitivity analysis indicates that the amount of hydrate formed in ASBs is strongly sensitive to the initial surface OC content of sediment and the reactivity parameter  $\nu$  in the reactive continuum model. The minimum and maximum values of  $\nu$  indicate a predominance of low- and high-reactivity OC compounds respectively, while intermediate values indicate a more uniform distribution of different OC compounds with depth. For higher reactivity parameters (for example,  $\nu > 0.3$ ), OC is exhausted rapidly in the upper sediment layers, where the anaerobic oxidation of methane dominates for the initial

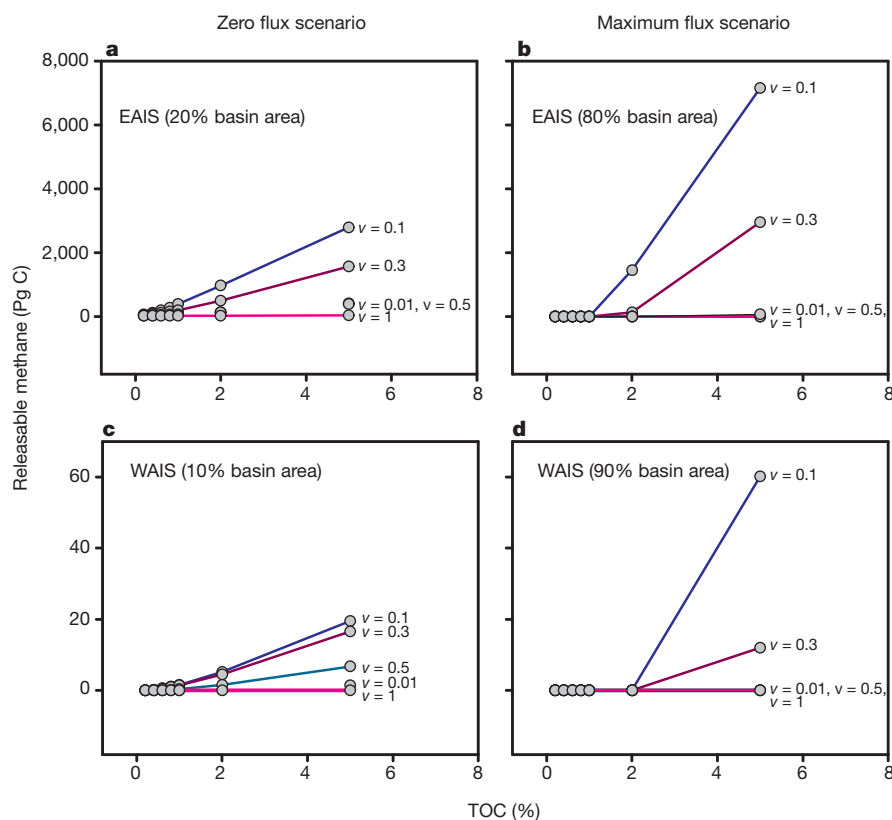


**Figure 2 | Methane hydrate+gas accumulation potential beneath the ice sheet.** This indicates the sensitivity of methane hydrate+gas accumulation ('releasable methane') beneath the Antarctic Ice Sheet to varying TOC(0,0) and  $\nu$  values in the reactive continuum model under the zero flux scenario for the EAIS (a) and WAIS (b), and the maximum flux scenario for the EAIS (c) and WAIS (d). Methane hydrate+gas accumulation is calculated after 30 Myr (EAIS) and 1 Myr (WAIS) of simulation time. The high hydrate inventory for the maximum flux scenario reflects the greater area contribution of melting basal conditions for the WAIS and EAIS.

16 kyr, while for low reactivity values (for example,  $\nu = 0.01$ ), slow rates of methanogenesis limit the amount of methane accumulation over million-year timescales. It is notable that intermediate values of  $\nu$  give the highest methane hydrate+gas accumulation under both the maximum and zero flux scenarios (Supplementary Information 3, Fig. 2). In these cases, higher TOC concentrations penetrate deeper into the sediment column and rates of degradation are sufficient to generate substantial methane. We conclude that the slow burn of organic matter over million-year timescales produces the most methane hydrate in Antarctic sediments.

Model results highlight that methane hydrate formation beneath the ice sheet is strongly controlled by basal temperature conditions (for example, wet bed versus frozen bed). Significant hydrate is only likely to be formed in sectors of ASBs with frozen basal conditions (the zero flux scenario) unless the OC content is relatively high (>2%) (Fig. 2). The latter may occur locally, as indicated in Antarctic Ocean Drilling Program core records containing ancient organic-rich material (Supplementary Fig. 3). In East Antarctica, long duration glaciation, aerially extensive ASBs and frozen basal conditions in some sectors may promote substantial hydrate accumulation (Fig. 2, Supplementary Information 1). Assuming two plausible end-member values for  $\nu$  (0.1 for typical marine sediments and 0.01 for highly recalcitrant OC typical of the deep rock biosphere; Supplementary Information 3a) and a surface TOC content of 1%, the model generates total hydrate+gas inventories of 70–390 Pg C for the EAIS (>90% as hydrate) (Fig. 2). Even if the duration of continuous ice cover in EAIS ASBs were shorter (for example, 5–10 Myr), it would still be possible to generate some hundreds of PgC of methane hydrate (Supplementary Fig. 6). Both end-member parameter sets give modelled surface and deep methane production rates ( $R_{\text{xn}}$ ) that compare well to those measured in marine sediments<sup>4–6</sup> and subglacial sediments (this paper and ref. 16) (Fig. 1b). The resulting hydrate is generated in ASBs with frozen conditions at the ice-sheet bed, occupying up to 30% pore space volume between 10 m and 100 m of the sediment surface (Fig. 3). The shallow depth of the latter contrasts with oceanic systems<sup>13</sup>, and reflects (1) the lack of a sulphate pool in the

upper sediment column after 16 kyr, designating methanogenesis as the terminal step for organic matter degradation, (2) no loss of methane at the sediment surface by diffusion and (3) lower methane solubility in shallow sediments. For the WAIS, shorter-duration glaciation and widespread melting conditions at the ice-sheet bed<sup>17</sup> result in zero methane hydrate formation in sediments for representative parameter sets (such as  $\nu = 0.01$ –0.1, TOC(0,0) = 1%), although there may be some local hydrate formation in association with organic-rich horizons (Fig. 2, Supplementary Tables 5 and 6).

Substantial parts of the WAIS contain sediment thicknesses of several kilometres (Supplementary Table 1) and exhibit enhanced geothermal heat flow and volcanism<sup>18</sup>. The thermal breakdown of organic matter or heavier hydrocarbons is common in marine basins with thick sediments and enhanced geothermal activity<sup>25</sup>. Hence, for the WAIS we consider the potential for thermogenic methanogenesis in deep sediments, with methane transported to the GHSZ by upward fluid flow. Because there is no sedimentation beneath the ice sheet (driving downward advection of sediments/porewaters), net upward fluid flow induced by geothermal heating is likely. We ran further model simulations for the WAIS (maximum flux scenario), applying a range of vertical fluid advection velocities representative of active geothermal sites (Supplementary Information 2f, and Fig. 4). Hydrate is produced throughout the entire GHSZ in simulations employing upward fluid flow velocities of just a few millimetres per year (Fig. 4). Typical upward fluid flow velocities at active vents and seeps exceed  $10 \text{ mm yr}^{-1}$  and can be  $2,500 \text{ mm yr}^{-1}$ , generating upward methane fluxes of over  $3 \text{ mol CH}_4 \text{ m}^{-2} \text{ yr}^{-1}$  (refs 26 and 27). However, this fluid flow has been shown to exhibit high spatial variability<sup>26</sup>. If geothermally active sites were present over 10% of the WAIS ASB area<sup>18</sup> and displayed low upward fluid flow rates ( $5 \text{ mm yr}^{-1}$ ) and more diffuse methane seepage ( $<1.0 \text{ mol m}^{-2} \text{ yr}^{-1}$ ), about 90 PgC of methane hydrate could be generated over 1 Myr (Fig. 4). If the geothermally active area reduced to 5% or 1% of the WAIS ASBs, then 47 PgC and 9 PgC of hydrate could be generated, respectively. Although they are speculative, these simulations indicate that it might be reasonable to expect local hydrate accumulations in WAIS ASBs.

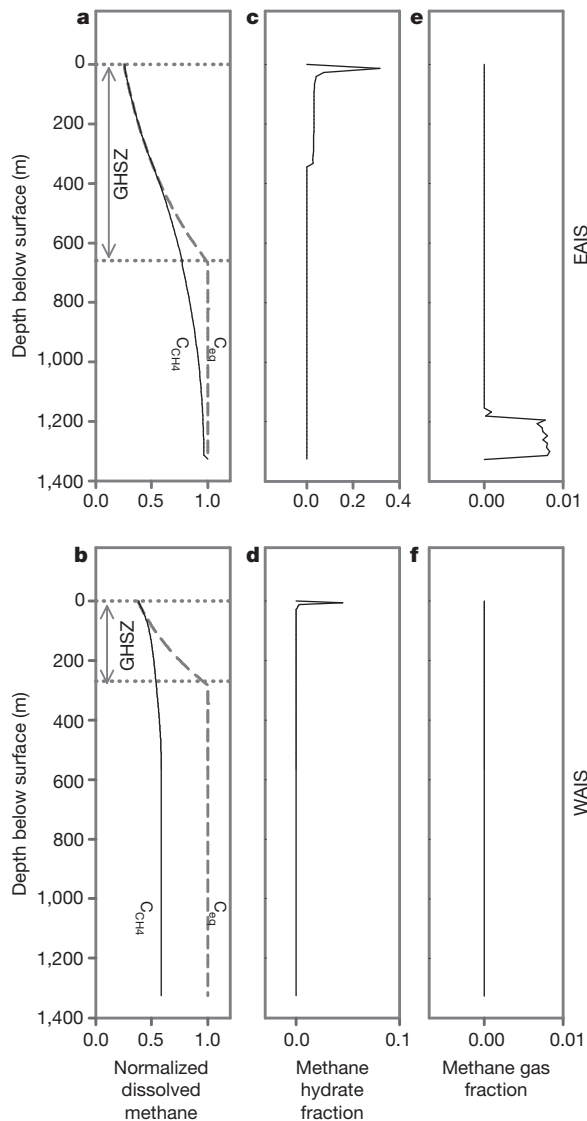


**Figure 3 | Vertical profiles of methane solubility, dissolved methane, methane hydrate and methane gas in zero flux simulations.** Concentrations in **a** and **b** are normalized to the maximum methane solubility defined at the three-phase equilibrium point for methane in pore waters  $C_{eq}$ , methane hydrate and methane gas are reported in units of percentage of pore volume (note the different scale for the x axis). Simulations assume 30 Myr (EAIS) and 1 Myr (WAIS) of glaciation. The upper and lower extent of the GHSZ is indicated.  $C_{eq}$  is the equilibrium concentration of methane in pore waters and  $C_{CH_4}$  is the modelled dissolved concentration of methane in pore waters.

Model results indicate that the potential hydrate reserve could be 70–390 PgC ( $1.31\text{--}7.28 \times 10^{14} \text{ m}^3$  methane gas) beneath the EAIS (biogenic production in frozen bed sectors) and some tens of PgC (about  $2 \times 10^{13} \text{ m}^3$  of gas) beneath the WAIS (thermogenic production in wet-based, geothermally active areas). This represents a sizeable reservoir of methane hydrate, of a similar order of magnitude to more recent estimates of Arctic permafrost and Arctic ocean hydrate reserves<sup>13</sup>, but lower than those calculated globally for marine sediments<sup>28</sup>. The size of the subglacial hydrate inventory is highly sensitive to ice thickness and likely to be located at shallow depths (Fig. 3), highlighting the strong potential for deglaciation to trigger hydrate destabilization via its effect on the ice overburden pressure (the pressure added by an ice column on top of sediments). For example, rapid ice-sheet thinning and retreat during previous collapses of the WAIS<sup>29</sup> might result in changes in the extent of the GHSZ and the destabilization of any methane hydrate, followed by release via venting, similar to

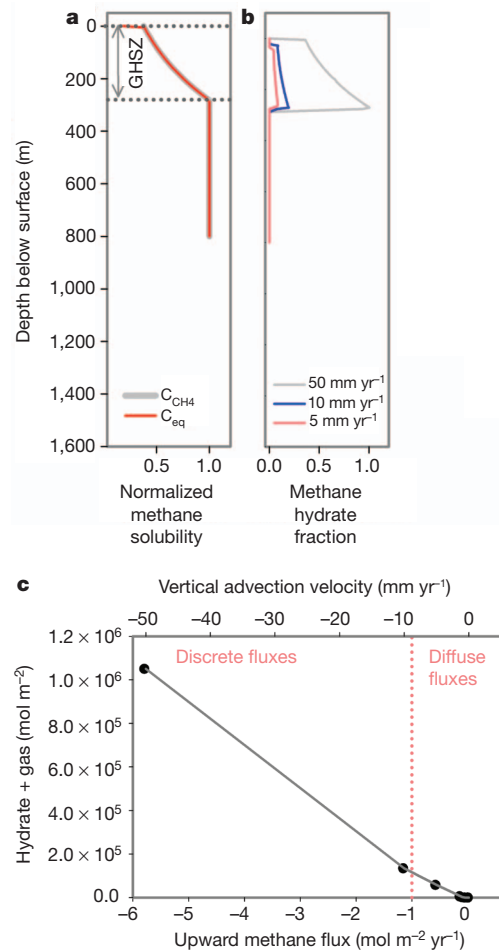


**Figure 4 | Modelled thermogenic methane accumulation beneath WAIS over 1 Myr of glaciation under the maximum flux scenario ( $v = 0.1$ ,  $\text{TOC}(0,0) = 1\%$ ).** **a**, Vertical profiles of methane solubility ( $C_{eq}$ ) and dissolved methane concentrations ( $C_{CH_4}$ , for a vertical advection velocity of 50  $\text{mm yr}^{-1}$  only) at  $t = 1 \text{ Myr}$  (that is, after a million years of glaciation) where concentrations are normalized to the maximum  $C_{eq}$ . The upper and lower extent of the GHSZ is indicated. **b**, Methane hydrate formed after 1 Myr of glaciation and employing different vertical advection velocities (in the range 5–50  $\text{mm yr}^{-1}$ ). Zones of upward fluid flow velocities and methane fluxes for active vents ('discrete fluxes') versus more diffuse seepage ('diffuse fluxes') are indicated based upon refs 26 and 27.

that occurring in the marine environment<sup>26</sup>. The impact of such methane hydrate destabilization upon atmospheric methane concentrations depends on the size, geographical distribution of the inventory and the pattern and rate of ice-sheet retreat. Ice-sheet retreat rates of the order of 1,000  $\text{km}^2 \text{ yr}^{-1}$  are possible for previous episodes of deglaciation (for example, the Laurentide retreat occurred at 1,200  $\text{km}^2 \text{ yr}^{-1}$ ; ref. 30). These rates might be exceeded in WAIS ASBs owing to the grounding of the ice sheet below sea level and the presence of weak tills, which promote the fast flow of ice and dynamic instability<sup>29</sup>. If we assume that just 15 PgC was present as methane hydrate over 10% of the WAIS ASB area ( $10^5 \text{ km}^2$ ), focused largely in marginal geothermally active zones<sup>18</sup>, ice retreat of 1,000  $\text{km yr}^{-1}$  could make 0.15 PgC  $\text{yr}^{-1}$  of hydrate available for release to the atmosphere. This slightly exceeds the atmospheric turnover rate of 0.13 PgC  $\text{yr}^{-1}$ , indicating its potential to affect atmospheric methane concentrations. For this to happen, hydrate destabilization would need to be a disequilibrium process, manifested by rapid methane transport to the sediment surface (for example, by venting<sup>26</sup>) at a rate that far exceeds that at which it can be oxidized. A hydrate inventory of the order of some tens of PgC in WAIS marginal basins seems plausible, based on

our model results, and is comparable to inventories for other localized marine hydrate reserves, for example, 15 Pg C of methane hydrate over 26,000 km<sup>2</sup> at Blake Ridge and 23 Pg C as hydrate at Hydrate Ridge, Cascadia Margin<sup>31</sup>.

We conclude that the Antarctic Ice Sheet could constitute a previously neglected component of the global methane hydrate inventory, although significant uncertainty exists. The predicted shallow depth of these reserves also makes them more susceptible to climate forcing than some other global hydrate reserves. If substantial methane hydrate and gas were present beneath the WAIS, hydrate destabilization during episodes of ice-sheet collapse could act as a positive feedback on global climate change during past and future ice-sheet wastage. Further validation of these assertions awaits deep drilling into ASBs via future international initiatives.

## METHODS SUMMARY

We use a well-established one-dimensional numerical hydrate model<sup>3</sup> (see Supplementary Information 2f), modified via the inclusion of an OC degradation model, based upon the reactive continuum approach<sup>23</sup>. Within this, methane production rates  $R_{\text{CH}_4}(z,t)$  are scaled to decreasing organic matter quality with sediment age, and hence depth. We assume physical properties for sediments similar to the properties previously used for ocean sediment modelling (listed in ref. 3). We prescribe an initial TOC depth profile of subglacial Antarctic marine sediments (TOC(z,0)) that is calculated from the steady-state solution of OC using the reactive continuum model and assuming a prescribed surface OC content, TOC(0,0) (Supplementary Information 3a), as well as an age/depth model, age(z). The age/depth model is constructed using a cubic spline interpolation of observed depth/age relationships in circum-Antarctic marine sediments<sup>32</sup>. See Supplementary Table 2 for site-specific parameters. We conduct a sensitivity analysis of hydrate accumulation to (1) OC content of sediments, (2) reactivity of organic matter in sediments, represented by  $\nu$  in the reactive continuum model, (3) initial saturation of methane in sediment pore waters at  $t = 0$  of the simulation, (4) ice thickness and (5) duration of glaciation (see Supplementary Information 2 and 3). Predictions of methane hydrate accumulation are made for representative parameter sets. Model results are scaled to estimates of total methane hydrate beneath the Antarctic Ice Sheet, assuming that ASBs underlie 50% of the WAIS area and 20% of the EAIS area. We assume that 10% of WAIS and 20% of EAIS ASBs exhibit frozen basal conditions at the sediment–ice interface, represented by our zero flux scenario in which no methane may diffuse out of the top of the sediment column. The remaining ASB areas are represented by our maximum flux scenario, in which methane is allowed to diffuse out of the top of the sediment column.

Received 10 October 2011; accepted 28 June 2012.

1. Prisco, J. *et al.* in *Polar Lakes and Rivers* (eds Vincent, W. F. & Laybourn-Parry, J.) 320 (Oxford University Press, 2009).
2. Ferraccioli, F., Armadillo, E., Jordan, T., Bozzo, E. & Corr, H. Aeromagnetic exploration over the East Antarctic Ice Sheet: a new view of the Wilkes Subglacial Basin. *Tectonophysics* **478**, 62–77 (2009).
3. Davie, M. K. & Buffett, B. A. A numerical model for the formation of gas hydrate below the seafloor. *J. Geophys. Res.* **106**, 497–514 (2001).
4. Wellsbury, P., Mather, I. & Parkes, R. J. Geomicrobiology of deep, low organic carbon sediments in the Woodlark Basin, Pacific Ocean. *FEMS Microbiol. Ecol.* **42**, 59–70 (2002).
5. Cragg, B. A. *et al.* Bacterial populations and processes in sediments containing gas hydrates (ODP Leg 146: Cascadia Margin). *Earth Planet. Sci. Lett.* **139**, 497–507 (1996).
6. Colwell, F. S. *et al.* Estimates of biogenic methane production rates in deep marine sediments at Hydrate Ridge, Cascadia margin. *Appl. Environ. Microb.* **74**, 3444–3452 (2008).
7. Parkes, R. J. *et al.* Bacterial biomass and activity in deep sediment layers from the Peru margin. *Phil. Trans. R. Soc. Lond. A* **331**, 139–153 (1990).
8. Yoshioka, H., Sakata, S., Cragg, B. A., Parkes, R. J. & Fujii, T. Microbial methane production rates in gas hydrate-bearing sediments from the eastern Nankai Trough, off central Japan. *Geochim. J.* **43**, 315–321 (2009).
9. Kotsyurbenko, O. R. *et al.* Acetoclastic and hydrogenotrophic methane production and methanogenic populations in an acidic West-Siberian peat bog. *Environ. Microbiol.* **6**, 1159–1173 (2004).
10. Franzmann, P. D., Roberts, N. J., Mancuso, C. A., Burton, H. R. & McMeekin, T. A. Methane production in meromictic Ace Lake, Antarctica. *Hydrobiologia* **210**, 191–201 (1991).
11. Smith, R., Miller, L. & Howes, B. The geochemistry of methane in Lake Fryxell, an amictic, permanently ice-covered, antarctic lake. *Biogeochemistry* **21**, 95–115 (1993).

12. Ellis-Evans, J. C. Methane in maritime Antarctic freshwater lakes. *Polar Biol.* **3**, 63–71 (1984).
13. Archer, D. Methane hydrate stability and anthropogenic climate change. *Biogeosciences* **4**, 521–544 (2007).
14. Wadham, J. L., Tranter, M., Tulaczyk, S. & Sharp, M. Subglacial methanogenesis: a potential climatic amplifier? *Glob. Biogeochem. Cycles* **22**, GB2021 (2008).
15. Lanoil, B. *et al.* Bacteria beneath the West Antarctic Ice Sheet. *Environ. Microbiol.* **11**, 609–615 (2009).
16. Boyd, E. S., Skidmore, M., Mitchell, A. C., Bakermans, C. & Peters, J. W. Methanogenesis in subglacial sediments. *Environ. Microbiol. Rep.* **2**, 685–692 (2010).
17. Pattyn, F. Antarctic subglacial conditions inferred from a hybrid ice sheet/ice stream model. *Earth Planet. Sci. Lett.* **295**, 451–461 (2010).
18. Maule, C. F., Purucker, M. E., Olsen, N. & Mosegaard, K. Heat flux anomalies in Antarctica revealed by satellite magnetic data. *Science* **309**, 464–467 (2005).
19. Claypool, G. F., Lorenson, T. D. & Johnson, C. A. Authigenic carbonates, methane generation, and oxidation in continental rise and shelf sediments, ODP leg 188, sites 1165 and 1166, offshore Antarctica (Prydz Bay). *Proc. ODP Sci. Results* **188**, 1–15 (2004).
20. Tarnocai, C. *et al.* Soil organic carbon pools in the northern circumpolar permafrost region. *Glob. Biogeochem. Cycles* **23**, GB2023 (2009).
21. Houghton, R. A. Balancing the global carbon budget. *Annu. Rev. Earth Planet. Sci.* **35**, 313–347 (2007).
22. Meyers, P. A. & Ishiwatari, R. Lacustrine organic geochemistry—an overview of indicators of organic matter sources and diagenesis in lake sediments. *Org. Geochem.* **20**, 867–900 (1993).
23. Boudreau, B. P. & Ruddick, B. R. On a reactive continuum representation of organic-matter diagenesis. *Am. J. Sci.* **291**, 507–538 (1991).
24. Reeburgh, W. S., Whalen, S. C. & Alperin, M. J. In *Microbial Growth on C1 Compounds* (eds Murrell, J. C. & Kelly, D. P.) 1–14 (Intercept Ltd, 1993).
25. Etiope, G. & Klusman, R. W. Geologic emissions of methane to the atmosphere. *Chemosphere* **49**, 777–789 (2002).
26. Torres, M. E. *et al.* Fluid and chemical fluxes in and out of sediments hosting methane hydrate deposits on Hydrate Ridge, OR. I: Hydrological provinces. *Earth Planet. Sci. Lett.* **201**, 525–540 (2002).
27. Wallmann, K., Drews, M., Aloisi, G. & Bohrmann, G. Methane discharge into the Black Sea and the global ocean via fluid flow through submarine mud volcanoes. *Earth Planet. Sci. Lett.* **248**, 545–560 (2006).
28. Boswell, R. & Collett, T. S. Current perspectives on gas hydrate resources. *Energy Environ. Sci.* **4**, 1206–1215 (2011).
29. Pollard, D. & DeConto, R. M. Modelling West Antarctic ice sheet growth and collapse through the past five million years. *Nature* **458**, 329–332 (2009).
30. Dyke, A. S., Prest, V. K. & Narraway, J. D. In *Map/Geological Survey of Canada 1702A* (Geological Survey of Canada, 1987).
31. Dickens, G. R., Paull, C. K. & Wallace, P. Direct measurement of in situ methane quantities in a large gas-hydrate reservoir. *Nature* **385**, 426–428 (1997).
32. Barker, P. F., Camerlenghi, A. & Acton, G. D. Leg 178 Summary. *Proc ODP Init. Rep.* **178**, 60 (1999).

**Supplementary Information** is linked to the online version of the paper at [www.nature.com/nature](http://www.nature.com/nature).

**Acknowledgements** This research was funded by the Natural Environment Research Council (UK—NERC grant NE/E004016/1) and the National Science Foundation WISSARD project (NSF-AISS 0839142). Support to J.L.W. was also provided by the Leverhulme Trust via a Phillip Leverhulme award and to S.A. by the Netherlands Organisation for Scientific Research (NWO). We acknowledge NSERC and Antarctica New Zealand for financial and logistic support for sampling in Antarctica and the Polar Continental Shelf Project for financial and logistic support for sampling in Arctic Canada. We thank S. Fitzsimons for assistance with sampling in Antarctica. A.D. was funded by an NSERC Undergraduate Student Research Award. This research used data provided by the Ocean Drilling Program. The Ocean Drilling Program is sponsored by the US National Science Foundation and participating countries under the management of the Joint Oceanographic Institutions, Inc. We thank C. Ruppel for comments on this manuscript.

**Author Contributions** J.L.W. wrote the paper and directed the work, and led the sample collection in Greenland. S.A. did the numerical modelling and contributed to manuscript preparation. S.T. assisted with the modelling and contributed to manuscript preparation. M.S. contributed to the writing of the manuscript and did experimental work. J.T. did the initial design of incubation experiments, laboratory analysis of incubation experiments, and sample collection. G.P.L. performed laboratory analysis of the incubation experiments, and did sample collection. E.L. performed laboratory analysis of incubation experiments. A.D. performed laboratory analysis of the incubation experiments. M.T. assisted with the manuscript and modelling calculations. M.J.S. added input to the incubation experiments, and did sample collection of Antarctic subglacial material. A.M.A. assisted with writing the manuscript and advised upon incubation experiments. A.R. assisted with manuscript preparation and numerical modelling. C.B. assisted with the laboratory analysis of the incubation experiments.

**Author Information** Reprints and permissions information is available at [www.nature.com/reprints](http://www.nature.com/reprints). The authors declare no competing financial interests. Readers are welcome to comment on the online version of this article at [www.nature.com/nature](http://www.nature.com/nature). Correspondence and requests for materials should be addressed to J.L.W. ([j.l.wadham@bris.ac.uk](mailto:j.l.wadham@bris.ac.uk)).